PALACKÝ UNIVERSITY IN OLOMOUC
FACULTY OF SCIENCE

OPTICAL REFERENCE GEOMETRY OF COMPACT OBJECTS SPACETIMES

ABSTRACT OF DOCTORAL THESIS

Branch: General Physics and Mathematical Physics
Supervisor: Prof. RNDr. Zdeněk Stuchlík, CSc.

JIŘÍ KOVÁŘ

OLOMOUC 2006

'Optical reference geometry of compact objects spacetimes'

Jiří Kovář
Institute of Physics, Faculty of Philosophy and Science, Silesian University in Opava
Bezručovo nám. 13, 746 01 Opava, Czech Republic

Abstract of Doctoral Thesis submitted for the scientific degree of Ph.D.
in General Physics and Mathematical Physics.
Faculty of Science, Palacký University in Olomouc
Supervisor: Prof. RNDr. Zdeněk Stuchlík, CSc.
September 2006

Typeset in LaTeX 2$_\varepsilon$

Contents

1. Introduction

Since 1916, Einstein's General theory of Relativity has been thought to be successful in explanation of gravitational phenomena as well as some conceptual questions of the 'old' Newtonian physics. We can recall the famous examples from the beginning of the 20th century, i.e., the gravitational deflection of light from distant stars passing close to the Sun, the precession of the Mercury perihelion and many others. Due to the Einstein theory, except such an 'earthbound' examples of a 'common' physics, we are now able to study fascinating black holes, hypothetical naked singularities† or related conception of 'time-travelling', wormholes and parallel universes. Of course, this puts up plenty of outstanding physical and philosophical questions and shows limits of our thinking and imagination, which many people are attracted by. 'Unfortunately', to comprehend these phenomena well, one must understand the gist of general relativity, i.e., the mathematical description of the curved spacetime and physics in it. And it does not have to be really easy.

Of course, because of the relative simplicity and elegance, the Newtonian approach to the dynamics is commonly used in the case of weak gravitational fields, where the inaccuracies of obtained results are negligible. But it fails in the case of strong gravitational fields near compact objects, such as astrophysically important neutron stars, black holes or naked singularities, where the most surprising events can happen. Wishing to investigate the physics in the vicinity of the compact objects, one must leave the Newtonian intuition and use the complex general relativistic approach, even in the basic case of test particles circular motion near the Schwarzschild black hole, described by the relatively simple Schwarzschild geometry.

But in 1988, in a way simpler and more demonstrative and understandable approach to the relativistic dynamics appeared. By an appropriate conformal (3+1) splitting of the Schwarzschild spacetime, the so-called optical reference geometry was defined [1]. It was demonstrated that this geometry enables us to define the gravitational and inertial forces in the framework of general relativity in accord with the Newtonian intuition. It means, the gravitational force is velocity independent and proportional to the gradient of a scalar function called 'gravitational potential', while the centrifugal force depends on the second power of velocity. Moreover, a particle motion can be described by using the forces in accordance with our Newtonian intuition [2], [3].

Thus anyone untrained in general relativistic dynamics, knowing only the form of these relativistic forces and basics of the Newtonian physics, can study a particle motion in strong gravitational fields in the relativistic way, quickly discovering 'unusual' effects

† In contrast to the black holes, the naked singularities are not covered by event horizons and thus the 'exotic' parts of the spacetimes near the singularity can 'communicate' with the distant universe. The Penrose conjecture of cosmic censorship suggests that no naked singularity can evolve from regular initial data, but the proof and even precise formulation of the conjecture is still a big challenge in general relativity. Therefore naked-singularity solutions of Einstein's equations related to the black-hole solutions should be considered as a possible explanation of quasars and active galactic nuclei.

taking place there. Effects like the reverse of orientation of the centrifugal force on the photon circular orbit, which becomes oriented inward the black hole at the radii less then the radius of the orbit. The centrifugal force vanishes at the radius of the photon circular orbit independently of the velocity; an observer located in a tunnel along this orbit can observe the 'straight' tunnel in front of him. Then it is natural for him that there is no centrifugal force acting on the particle moving along the orbit (see Fig. 1). Generally, the centrifugal force defined in the framework of the optical geometry vanishes in all the particle trajectories coalescing with the light geodesics, i.e., geodesics of the optical reference geometry coincide with the trajectories of light. Hence, no 'curvature' of the trajectory from the point of view of optical geometry means no centrifugal force. Therefore the geometry was called optical reference geometry.

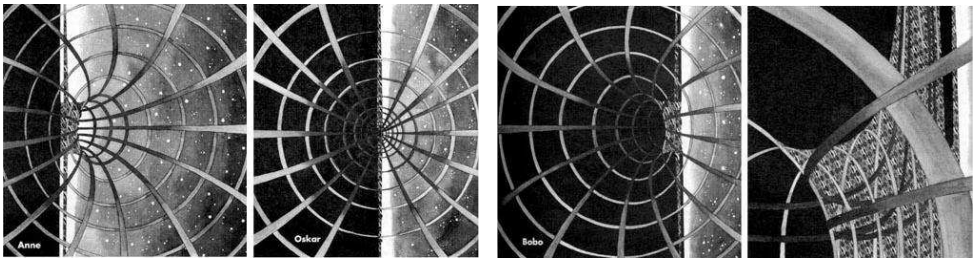

Figure 1. Three concentric circular 'tunnels' in the equatorial plane of the Schwarzschild black hole from the point of view of three astronauts located in. Curved photon trajectories cause the 'unusual' view of the astronauts. Anne is located in the tunnel above the photon circular orbit (first part of the figure). Her tunnel looks curved 'naturally'. Oskar is located in the tunnel along the photon circular orbit (second part) and his tunnel seems to be straight. Bobo is in the tunnel under the photon circular orbit (third part) and his tunnel seems to be curved contrariwise. The detail of the tunnel is shown in the last part of the figure.

Of course, the Schwarzschild black-hole spacetimes can describe only a narrow part of the compact objects spectrum. However, it was shown that the definition of the optical reference geometry and related inertial forces can be generalized, extending its applicability to any type of stationary spacetimes [4], [6], and even non-stationary spacetimes [7], [8]. Then, the optical reference geometry and inertial forces formalism were investigated in spacetimes around astrophysically more relevant classes of compact objects, such as charged or rotating black holes, described by the static and spherically symmetric Reissner-Nordström solution [11] or stationary and axially symmetric Kerr solution [13], [14], eventually around both the charged and rotating black holes and naked singularities, described by the Kerr-Newman solution [15].

Since the late 20th century, the cosmological observations have shown the accelerated expansion of our universe. The explanation of this effect, supported by wide range of cosmological tests (analysis of the cosmic microwave background, measurements of the distances of high red-shifted galaxies using the supernovas, investigation of the quasar gravitation lensing, etc.) can be found within the inflation cosmology. The accelerated

expansion is thought to be caused by the 'nonzero vacuum energy' described by the nonzero positive value of the cosmological constant Λ, or by influence of the similarly behaved new form of energy called 'quintessence', whereas both the possibilities are usually called 'dark energy'. The presence of the 'relic' repulsive positive cosmological constant with the expected value $\Lambda \sim 10^{-56}$ cm^{-2} then leads to some important astrophysical consequences [21].

Investigation of the optical reference geometry and inertial forces formalism for all the mentioned black-hole and naked-singularity spacetimes considered with the additional contribution of the repulsive cosmological constant, i.e., for the Schwarzschild-de Sitter [9], [39], Reissner-Nordström-de Sitter [12] or Kerr-de Sitter [26], [29] spacetimes, has shown many interesting phenomena. Of course, the situation is much more complicated in these spacetimes, compared to the case of the pure Schwarzschild spacetime. Remind that the most general Kerr-Newman-de Sitter spacetimes allow existence of even three event horizons. Behaviour of the forces is complex, incorporating influence of all the background parameters on the particle motion. There are more points of their vanishing, changing orientation and extrema. It was shown that some properties of the relativistic dynamics can be visualized by using the embedding diagrams, the useful relativistic tool. In the case of the optical reference geometry, the shape of the embedding diagrams is closely related to the behaviour of the centrifugal force. Turning points of the embedding diagrams are located exactly at the radii where the centrifugal force acting on the particle moving along the circular orbit vanishes independently of the velocity [16], [17], [18]. In the case of the static spacetimes, such radii coincide with the radii of photon circular orbits. Unfortunately, in the stationary (non-static) spacetimes, the radii where the centrifugal force vanishes independently of the velocity do not correspond to the radii of photon geodesics. Thus the original property of the optical reference geometry implicative the name of the geometry disappears. Moreover, in general, the optical reference geometry can not be entirely embeddable and the embedding diagrams then consist from several parts.

In spite of it, we can state that the optical reference geometry and the related inertial forces formalism present an illustrative alternative to the standard general relativistic approach, practically and intuitively applicable [19], [20], [29], allowing us to treat the general relativistic effects in terms of the concepts known from the Newtonian mechanics.

2. Fundamental definitions of the formalism

The initial Abramowicz definition of the optical reference geometry and inertial forces [1] and its subsequent generalization [4] and [6] have shown that the formalism can be defined in general spacetimes lacking any symmetry. However, as for the practical usage, the formalism is useful mainly in the astrophysically relevant case of the circular motion in the stationary and axially symmetric or static and spherically symmetric spacetimes.

2.1. General case

In stationary spacetimes described by a metric g_{ik}†, the definition of the optical reference geometry and inertial forces formalism is based on introducing of family of special observers with a timelike, unit and hypersurface orthogonal 4-velocity field n^i, and with its 4-acceleration field equal to the gradient of a scalar function [6], i.e.,

$$n^k n_k = -1, \quad n_{[i}\nabla_j n_{k]} = 0, \quad n^i \nabla_i n_k = \nabla_k \Phi. \tag{1}$$

Such a vector field can be chosen in the form

$$n^i = e^{-\Phi}\iota^i, \quad \Phi = \frac{1}{2}\ln(-\iota^i \iota_i), \tag{2}$$

whereas the vector field ι_i corresponds to a hypersurface orthogonal timelike vector field parallel to n^i.

The vector field n^i is not uniquely determined by relations (1), however, locally each particular choice of n^i uniquely defines a foliation of a spacetime into slices, each of which represents the space of the special observers at a particular instant of time. The geometry of the instantaneous 3-dimensional space (hypersurface) is described by the metric

$$h_{ik} = g_{ik} + n_i n_k, \tag{3}$$

the so-called directly projected geometry. Its conformally adjusted metric

$$\tilde{h}_{ik} = e^{-2\Phi} h_{ik} \tag{4}$$

is then the so-called *optical reference geometry*.

Considering now a test particle with a rest mass m, we can decompose its 4-velocity u^i by using the relation

$$u^i = \gamma(n^i + v\tau^i), \tag{5}$$

where n^i is the 4-velocity of the special observers, τ^i is the unit spacelike vector orthogonal to it along which the spatial 3-velocity with the magnitude v is aligned. The quantity $\gamma = (1 - v^2)^{-1/2}$ is the Lorentz normalization factor that makes $u^i u_i = -1$. Moreover, there is $\gamma = -n^i u_i$, $\gamma v \tau^i = u^k h^i_k$, where $h^i_k = \delta^i_k + n^i n_k$ is the projection tensor allowing us to project the 4-vectors into the 3-dimensional hypersurface.

† The metric of signature +2, geometrical units ($c = G = 1$) and latin indexies taking values from 0 to 3, corresponding later to the coordinates (t, r, ϕ, θ), are used.

By using the spacelike unit vector parallel to τ^i in the optical reference geometry, i.e., the vector $\tilde{\tau}^i = e^{\Phi}\tau^i$, its covariant form $\tilde{\tau}_i = e^{-\Phi}\tau_i$, the scalar $\tilde{E} = -\iota^i u_i = \gamma e^{\Phi}$ (pseudo-energy), identity $\gamma^2 = 1 + v^2\gamma^2$ and the condition of hypersurface orthogonality, and by denoting $\tilde{v} = \gamma v$, the projection of the 4-acceleration $a_k = u^i \nabla_i u_k$ into the 3-dimensional hypersurface can be written as

$$a_j^{\perp} = h_j^k a_k = \nabla_j \Phi + \tilde{v}^2 \tilde{\tau}^i \tilde{\nabla}_i \tilde{\tau}_j + \gamma^2 v X_j + \dot{V}\tilde{\tau}_j, \tag{6}$$

where $X_j = n^i(\nabla_i \tau_j - \nabla_j \tau_i)$ and $\dot{V} = u^i \nabla_i (\tilde{E} v)$.

The real force acting on a particle (for example, a rocket engine thrust) can be defined by relation $F_k = ma_k$ and projected into the hypersurface. The motion equation of the particle in its own co-moving frame can be then written as

$$F_k{}^{\perp} - ma_k^{\perp} = 0, \tag{7}$$

which suggests that the particle is not accelerated in this frame. The real force $F_k^{\perp}$ is balanced by the inertial force $F'^{\perp}_k$, which can be advantageously decomposed into four parts, i.e.,

$$F'^{\perp}_k = -ma_k^{\perp} = G_k + Z_k + C_k + E_k, \tag{8}$$

where

$$G_k = -m\nabla_k \Phi, \tag{9}$$

$$Z_k = -m\tilde{v}^2 \tilde{\tau}^i \tilde{\nabla}_i \tilde{\tau}_k, \tag{10}$$

$$C_k = -m\gamma^2 v X_k, \tag{11}$$

$$E_k = -m\dot{V}\tilde{\tau}_k. \tag{12}$$

Due to the properties of the forces, it is possible to consider them to be counterparts of the gravitational G_k, centrifugal Z_k, Coriolis C_k and Euler E_k forces familiar from the Newtonian physics.

2.2. Axially symmetric spacetimes

In stationary and axially symmetric spacetimes with the axis of symmetry oriented along the latitudinal coordinate $\theta = 0$, where $\eta^i = \delta^i_t$ and $\xi^i = \delta^i_\phi$ are the Killing vector fields, it is easy to check that the vector field

$$n^i = e^{-\Phi}(\eta^i + \Omega_{LNRF}\xi^i), \tag{13}$$

$$\Phi = \frac{1}{2}\ln\left[-(\eta^i + \Omega_{LNRF}\xi^i)(\eta_i + \Omega_{LNRF}\xi_i)\right], \tag{14}$$

where $\Omega_{LNRF} = -\eta^i\xi_i/\xi^i\xi_i$, defines the family of special observers (2). In this case, they correspond to the locally non-rotating observers, moving along circular orbits with the angular velocity $d\phi/dt = \Omega_{LNRF}$ [6]‡.

‡ In static and spherically symmetric spacetimes, there is $\eta^i\xi_i = 0$. Thus $\Omega_{LNRF} = 0$, the vector field $\iota^i \equiv \eta^i$ and n^i corresponds to the 4-velocity field of the static observers

3. Kerr-de Sitter spacetimes

Kerr-de Sitter (KdS) spacetimes are stationary and axially symmetric solutions of Einstein's equations with a positive cosmological constant. KdS geometry describes spacetimes around isolated, rotating and uncharged black holes or naked singularities in the universe with a repulsive cosmological constant. Thus the spacetimes are suitable for the description of phenomena around giant black holes in quasars and active galactic nuclei. The KdS spacetimes are characterized by three parameters: by the mass M and rotational a parameter of the source, and by the cosmological constant Λ. Because of the interplay of the parameters, the structure of the spacetimes is relatively complicated.

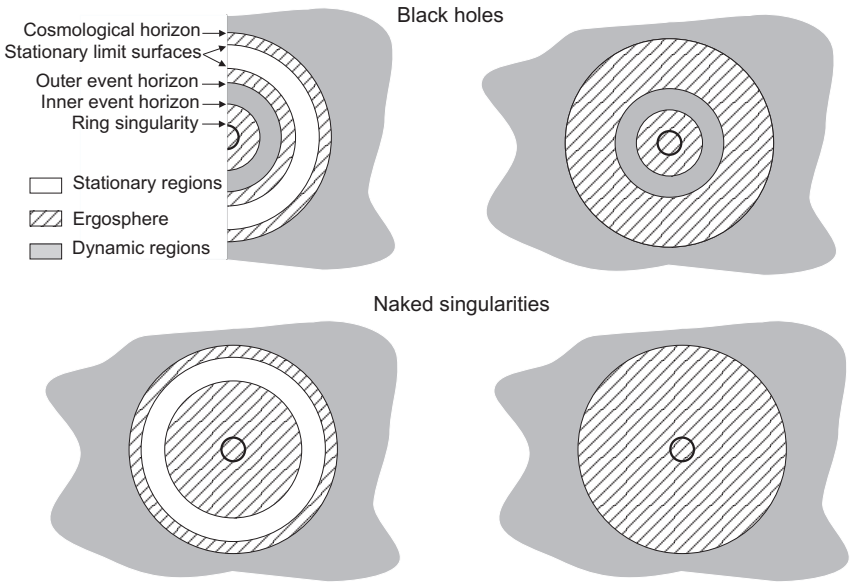

Figure 2. Different types of the KdS spacetimes (sketches of equatorial planes), differing in the number of horizons (stationary regions) and static limit surface (ergospheres).

3.1. The geometry

In standard Boyer-Lindquist coordinates $x^i = (t, r, \phi, \theta)$, the line element of the KdS geometry is given by the relation

$$ds^2 = -\frac{\Delta_r}{I^2\rho^2}(dt - a\sin^2\theta d\phi)^2 + \frac{\Delta_\theta \sin^2\theta}{I^2\rho^2}[adt - (r^2+a^2)d\phi]^2 + \frac{\rho^2}{\Delta_r}dr^2 + \frac{\rho^2}{\Delta_\theta}d\theta^2, \tag{15}$$

where

$$\Delta_r = r^2 - 2Mr + a^2 - \frac{1}{3}\Lambda r^2(r^2+a^2), \tag{16}$$

$$\Delta_\theta = 1 + \frac{1}{3}\Lambda a^2\cos^2\theta, \tag{17}$$

$$I = 1 + \frac{1}{3}\Lambda a^2, \tag{18}$$

$$\rho^2 = r^2 + a^2\cos^2\theta. \tag{19}$$

It is convenient to introduce the dimensionless cosmological parameter

$$y = \frac{1}{3}\Lambda M^2. \tag{20}$$

For simplicity, we put $M = 1$ hereafter, thus also the coordinates t, r, the line element ds, and the parameter a become dimensionless.

For $a \neq 0$, $y = 0$, we obtain the line element for the Kerr geometry [14], [34], for $a = 0$, $y > 0$, the Schwarzschild-de Sitter (SdS) geometry [9], [39] and for $a = 0$, $y = 0$, the well known Schwarzschild geometry [34]. The KdS spacetimes, being stationary and axially symmetric, admit both the Killing vector fields η^i and ξ^i, which are not globally orthogonal, i.e., $\eta^i\eta_i = g_{tt}$, $\xi^i\xi_i = g_{\phi\phi}$ and $\eta^i\xi_i = g_{t\phi}$. The only intrinsic singularity of the KdS solution is the ring singularity in the equatorial plane given by the relation $\rho = 0$.

3.2. Black holes and naked singularities

The pseudo-singularities of the KdS solution are given by the relation

$$\Delta_r(r; a^2, y) = 0, \tag{21}$$

determining the event horizons. In dependence on the values of the spacetime parameters a^2 and y, the KdS black-hole spacetimes contain even three event horizons, separating dynamic and stationary regions of the spacetimes. Along with the black-hole solutions of Einstein's equations also the naked-singularity solutions with the only horizon appear (see Fig. 2, [29], [24]). For given values of a^2 and y, the radii of the horizons are due to relation (21) determined by solutions of the equation

$$a^2 = a_h^2(r; y) \equiv \frac{r^2 - 2r - yr^4}{yr^2 - 1}. \tag{22}$$

In the case of the Kerr spacetimes, for $a^2 \leq 1$, there exist black-hole spacetimes with two event horizons separating the dynamic region between two stationary regions. The naked-singularity spacetimes with no horizons and the only stationary region exist for $a^2 > 1$. In the case of the SdS spacetimes, there exist only black-hole spacetimes for $y \leq 1/27$ with the only event horizon separating the stationary and dynamic regions, whereas for $y > 1/27$, the SdS spacetimes are dynamic naked-singularity spacetimes. The Schwarzschild spacetimes, characterized by the only parameter contain always one black-hole horizon at the radius $r = 2$, beyond which the spacetime is dynamic.

3.3. Static radii

The repulsive character of the cosmological constant enables existence of the so-called static radii, where the gravitation attraction of the source is just balanced by the cosmological repulsion [41]. The static radii in the equatorial plane and on the axis of symmetry of the KdS spacetimes correspond to the radii of static equilibrium positions of the spinless particles [24].

In the equatorial plane of the KdS spacetimes, the static radius is located at

$$r = r_{sr} \equiv y^{-1/3}. \tag{23}$$

On the axis of symmetry, there are at most two static radii† dependent on both the spacetime parameters a^2 and y. For given values of the parameters, the static radii are determined by solutions of the equation

$$a^2 = a^2_{sr}(r; y) \equiv \frac{-1 - 2r^3 y + \sqrt{1 + 8r^3 y}}{2ry}. \tag{24}$$

In the case of the Kerr spacetimes, there are no static radii in the black-hole spacetimes neither in the equatorial plane nor on the axis of symmetry, but in the naked-singularity spacetimes, one static radius appears on the axis. In the case of the SdS spacetimes, there is one static radius at $r_{sr} = y^{-1/3}$, of course, due to the spherical symmetry, for any value of θ. In the Schwarzschild spacetime, there is no static radius.

3.4. Static limit surfaces and ergosphere

Because of the rotation of the source, the dragging of the spacetimes and ergosphere takes place in the KdS spacetimes. The ergosphere satisfies the condition $g_{tt} > 0$, and it is split and limited by the static limit surfaces, determined by the relation $g_{tt} = 0$ and event horizons or by the singularity‡ [24]. In the equatorial plane of the KdS spacetimes, radii of the static limit surfaces r_{sl-} (inner) and r_{sl+} (outer) are given by solutions of the equation

$$a^2 = a^2_{sl}(r; y) \equiv \frac{r - 2 - yr^3}{yr}. \tag{25}$$

On the axis of symmetry, the static limit surfaces coalesce with the horizons, i.e., they are determined by the function $a^2_h(r; y)$ and thus there is no ergosphere here.

In the equatorial plane of the Kerr spacetimes, there is the only static limit surface located at $r = 2$ independently of a^2, whereas on the axis of symmetry, the surface coalesces with the outer event horizon and thus there is no ergosphere. Naturally, in the case of the SdS and Schwarzschild spacetimes, the static limit surfaces and ergosphere do not exist there.

---

† In fact, the number of static equilibrium positions of spinless particles on the axis of symmetry is always double of the mentioned number of static radii, taking both the parts of the axis $\theta = 0$ and $\theta = \pi$ into account, and using the Kerr-Schild (Cartesian) coordinate $z = r\cos\theta$. In this sense, in the equatorial plane, there is infinity number of static equilibrium positions related to one static radius, which correspond to different values of the azimuthal coordinate ϕ.

‡ Mostly (but not in the thesis), the ergosphere is consider to be only a part of the region where $g_{tt} > 0$. Namely the part located in the outer stationary black-hole region only. We denote all the stationary regions where $g_{tt} > 0$ as the ergosphere. Moreover, if it is not explicitly mentioned, we do not consider the static limit surfaces coalescent with the event horizons or singularity into account and classification.

3.5. Classification

According to the presented characteristics, the KdS spacetimes can be divided into six classes differing in the number of the event horizons, static limit surfaces and static radii in the equatorial plane and on the axis of symmetry (see Tab. 1 and Fig. 3.).

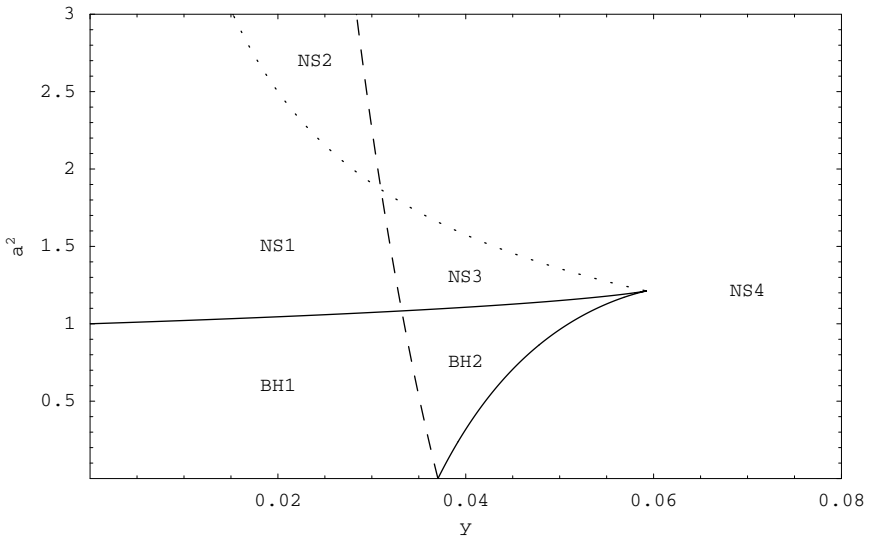

Figure 3. Classification of the KdS spacetimes. The parametric plane (a^2, y) is divided into regions corresponding to classes BH1-NS4 differing in the number of event horizons, static limit surfaces and static radii in the equatorial plane and on the axis of symmetry.

Table 1. Classification of KdS spacetimes according to the number of horizons, static limit surfaces, static radii in the equatorial plane and on the axis of symmetry. In each column, the first of two digits denotes the number in the equatorial plane, the second one on the axis of symmetry.

Class	**event horizons**	**static limit surfaces**	**static radii**
BH1	3,3	2,3	1,1
BH2	3,3	0,3	0,1
NS1	1,1	2,1	1,2
NS2	1,1	2,1	1,0
NS3	1,1	0,1	0,2
NS4	1,1	0,1	0,0

4. Behaviour of forces

As well as in the Newtonian physics, the inertial forces are defined by means of the particle acceleration. Hypersurface orthogonal projection of the 4-acceleration can be decomposed into four different parts. Thus here, in contrast to the Newtonian physics, the gravitational force as the first part of the decomposition ranks among the inertial forces. In general, the gravitational force exists due to the 4-acceleration of the reference frame of the special observers, as required in the equivalence principle.

Furthermore, we can summarize that all the forces (9)-(12) are defined in the co-moving frame of the particle with 4-velocity u^i, in contrast to the velocity of the particle v which is measured by the special observers with the 4-velocity n^i. In the case of $u^i = n^i$, the co-moving and reference frames coincide and $v = 0$. Thus the only non-vanishing inertial force is the gravitational force. It is proportional to the gradient of the function Φ, which does not depend on the intrinsic properties of test particles and their velocities. Therefore Φ is considered as a generalization of the Newtonian potential. The centrifugal force depends on the second power of the velocity, which corresponds to its Newtonian counterpart, and the Coriolis force depends on the first power of the velocity and vanishes in static spacetimes. The Euler force has no direct Newtonian counterpart.

Of course, such properties of the forces, namely the understandable 'Newtonian' form, provide the alternative and intuitive description of the relativistic dynamics (see Section 5). Moreover, choosing a characteristic type of motion and knowing the related behaviour of the forces, we can also understand the influence of the spacetime parameters on the relativistic dynamics. There are many astrophysical and conceptual reasons to choose the circular motion of a particle at fixed radius and latitude. Then the 4-velocity of the particle is given by the relation

$$u^i = e^{-A}(\eta^i + \Omega\xi^i), \tag{26}$$

$$A = \frac{1}{2}\ln\left[-(\eta^i + \Omega\xi^i)(\eta_i + \Omega\xi_i)\right], \tag{27}$$

where Ω is angular velocity of the particle. Since the circular motion is directed along the Killing vector field ξ^i, there is

$$\tau^i = (\xi^k\xi_k)^{-1/2}\xi^i. \tag{28}$$

Now, the Lorentz factor γ and magnitude of the velocity v (orbital velocity in this case) are given due to expressions (5) and (26) by the relations

$$\gamma = e^{\phi - A}, \quad v = e^{-\Phi}(\xi^i\xi_i)^{1/2}(\Omega - \Omega_{LNRF}), \tag{29}$$

and the components of the inertial forces (9)-(12) are given by the relations

$$G_k = -m\,\nabla_k\Phi, \tag{30}$$

$$Z_k = m(\gamma v)^2\,\frac{1}{2}(\xi^i\xi_i)^{-1}e^{-2\Phi}[e^{2\Phi}\nabla_k(\xi^i\xi_i) - \xi^i\xi_i\nabla_k(e^{2\Phi})], \tag{31}$$

$$C_k = m\gamma^2 v\,(\xi^i\xi_i)^{-3/2}e^{-\Phi}[\xi^i\xi_i\nabla_k(\eta^i\xi_i) - \eta^i\xi_i\nabla_k(\xi^i\xi_i)], \tag{32}$$

$$E_k = m\,e^{\Phi}\gamma^3 u^i\nabla_i(v)\tilde{\tau}_k. \tag{33}$$

Of course, time and azimuthal coordinates of the gravitational, centrifugal and Coriolis forces vanish. On the other hand, in the case of the Euler force, radial and latitudinal coordinates vanish.

For the further investigation of the relativistic dynamics, it is convenient to rewrite the inertial forces into the form

$$G_k = m\,\mathcal{G}_k, \tag{34}$$

$$Z_k = m\tilde{v}^2\,\mathcal{Z}_k, \tag{35}$$

$$C_k = m\tilde{v}(1-\tilde{v}^2)^{1/2}\,\mathcal{C}_k, \tag{36}$$

$$E_k = m(1-\tilde{v}^2)^{3/2}\,\mathcal{E}_k, \tag{37}$$

where $\mathcal{G}_k$, $\mathcal{Z}_k$, $\mathcal{C}_k$ and $\mathcal{E}_k$ are mass and velocity independent parts of the inertial forces, i.e., velocity independent parts of the related accelerations. Due to their behaviour, the forces can vanish at some radii and latitudes independently of the velocity and change their signs.

4.1. Equatorial motion in Kerr-de Sitter spacetimes

In the case of the uniform equatorial motion ($v = const$, $\theta = \pi/2$), latitudinal components of all the forces vanish. Moreover, the Euler force vanishes in the case of the uniform circular motion completely. The only non-vanishing radial components of the velocity independent parts of the accelerations take in the KdS spacetimes form

$$\mathcal{G}_r(r;a^2,y) = \{r\Delta_r[ra^4y + (yr^3+r+2)a^2 + r^3]\}^{-1}\{r^3a^2(a^2+r^2)^2y^2 + r^2(a^2+r^2)[r^3+a^2(r+4)]y - r^4 - 2r^2a^2 + 4ra^2 - a^4\}, \tag{38}$$

$$\mathcal{Z}(r;a^2,y) = \{r\Delta_r[ra^4y + (yr^3+r+2)a^2 + r^3]\}^{-1}\{r^3a^4(a^2+r^2)y^2 + r^2a^2 \times [(2r+5)a^2 + r^2(2r+3)]y + r^4(r-3) + ra^2[r(r-3)+6] - 2a^4\}, \tag{39}$$

$$\mathcal{C}_r(r;a^2,y) = \frac{2a(a^2+3r^2)}{r\sqrt{\Delta_r}\,[ra^4y + (yr^3+r+2)a^2 + r^3]}. \tag{40}$$

It is immediately clear that $\mathcal{C}_r(r;a^2,y)$ does not vanish, in contrast to $\mathcal{G}_r(r;a^2,y)$ and $\mathcal{Z}_r(r;a^2,y)$ §.

§ For comparison, in the case of the uniform equatorial circular motion in the Schwarzschild spacetime, there are only radial components of the gravitational and centrifugal forces non-vanishing, determined by the relations

$$G_r = m\mathcal{G}_r = -m\,\frac{1}{r^2-2r},$$

$$Z_r = m(\gamma v)^2\mathcal{Z}_r = m(\gamma v)^2\,\frac{r-3}{r^2-2r},$$

Of course, the centrifugal force vanishes for $v = 0$ at all the radii, but it also vanishes independently of the velocity at the radii where the velocity independent part of the acceleration vanishes, i.e., at the radius $r = 3$. It is the radius where the centrifugal force changes its orientation, being repulsive (positive) at the radii $r > 3$ and attractive (negative) at the radii $r < 3$, which does not occur in weak gravitational fields (see Fig. 5).

4.2. Classification

The KdS spacetimes can be classified according to the number of circular orbits where the gravitational force vanishes and orbits where the centrifugal forces vanishes independently of the velocity (see Tab. 2 and Fig. 4). The behaviour of the related velocity independent parts of the accelerations are illustrated in Fig. 6.

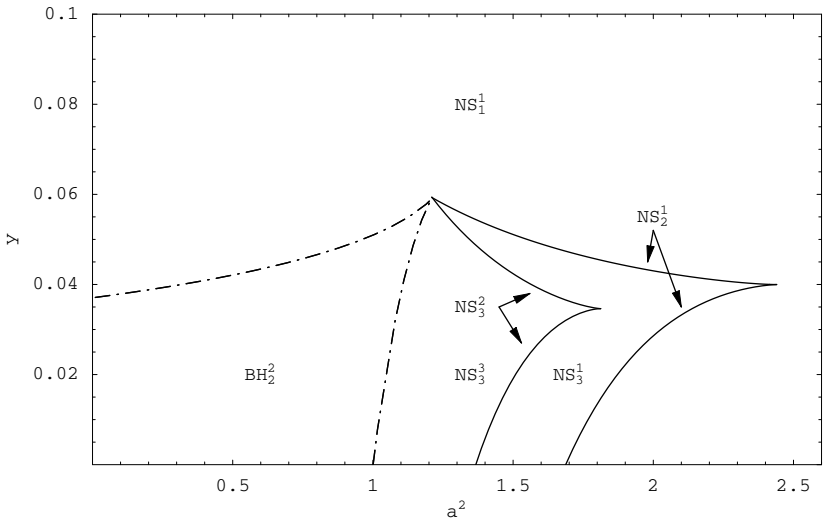

Figure 4. Classification of the KdS spacetimes. The parametric plane (a^2, y) is divided into regions corresponding to the classes differing in the number of circular orbits where $\mathcal{G}_r(r; a^2, y) = 0$ (subscript) and orbits where $\mathcal{Z}_r(r; a^2, y) = 0$ (superscript).

Table 2. Classification of the KdS (Kerr and SdS and Schwarzschild) spacetimes according to the number of circular orbits where the gravitational force vanishes (subscript) and orbits where the centrifugal force vanishes independently of the velocity (superscript).

	BH spacetimes	**NS spacetimes**
KdS	BH_2^2	NS_1^1, NS_2^1, NS_3^1, NS_3^2, NS_3^3
Kerr	BH_1^2	NS_0^1, NS_1^1, NS_2^1, NS_2^2, NS_2^3
SdS	BH_1^1	—
Schw	BH_0^1	—

- KdS black-hole spacetimes contain only one circular orbit where the gravitational force vanishes, and only one orbit where the centrifugal force vanishes independently of the velocity in each of the stationary regions. Both the gravitational and centrifugal forces change their orientations on these orbits. The same number of the orbits appears in the Kerr black-hole spacetimes, except for the outer stationary region, where there is no circular orbit where the gravitational force vanishes. The SdS black-hole spacetimes contain only one orbit where the gravitational force vanishes and one circular orbit where the centrifugal force vanishes independently of the velocity. The Schwarzschild spacetimes contains one orbit where the centrifugal force vanishes independently of the velocity and none orbit where the gravitational force vanishes.

- KdS naked-singularity spacetimes can contain even three circular orbits where the gravitational force vanishes and other three orbits where the centrifugal force vanishes independently of the velocity, which indicates a relatively complex structure of these spacetimes as a result of mixed influence of the rotation of the source and the cosmological repulsion. The Kerr naked-singularity spacetimes contain at maximum only two circular orbits where the gravitational force vanishes, but there are at most three circular orbits where the centrifugal force vanishes independently of the velocity in accord with the case of the KdS naked-singularity spacetimes. With parameters a and y growing, the structure of the forces simplifies. There are one orbit with vanishing of the centrifugal force and the other with vanishing of the gravitational force.

Of course, the additional orbit in the KdS (SdS) spacetimes compared to the Kerr (Schwarzschild) spacetimes is due to the cosmological repulsion.

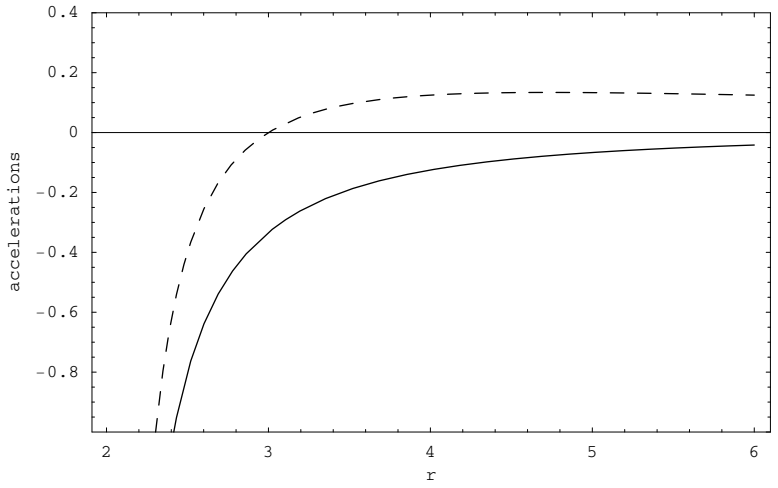

Figure 5. Gravitational acceleration $\mathcal{G}_r(r)$ (solid) and velocity independent part of the centrifugal acceleration $\mathcal{Z}_r(r)$ (dashed) of particles moving along circular orbits in the equatorial plane of the Schwarzschild spacetimes. Positive (negative) parts of $\mathcal{Z}_r(r)$ determine repulsive (attractive) centrifugal force oriented outwards (towards) the singularity at $r = 0$. The gravitational force is attractive at all the radii.

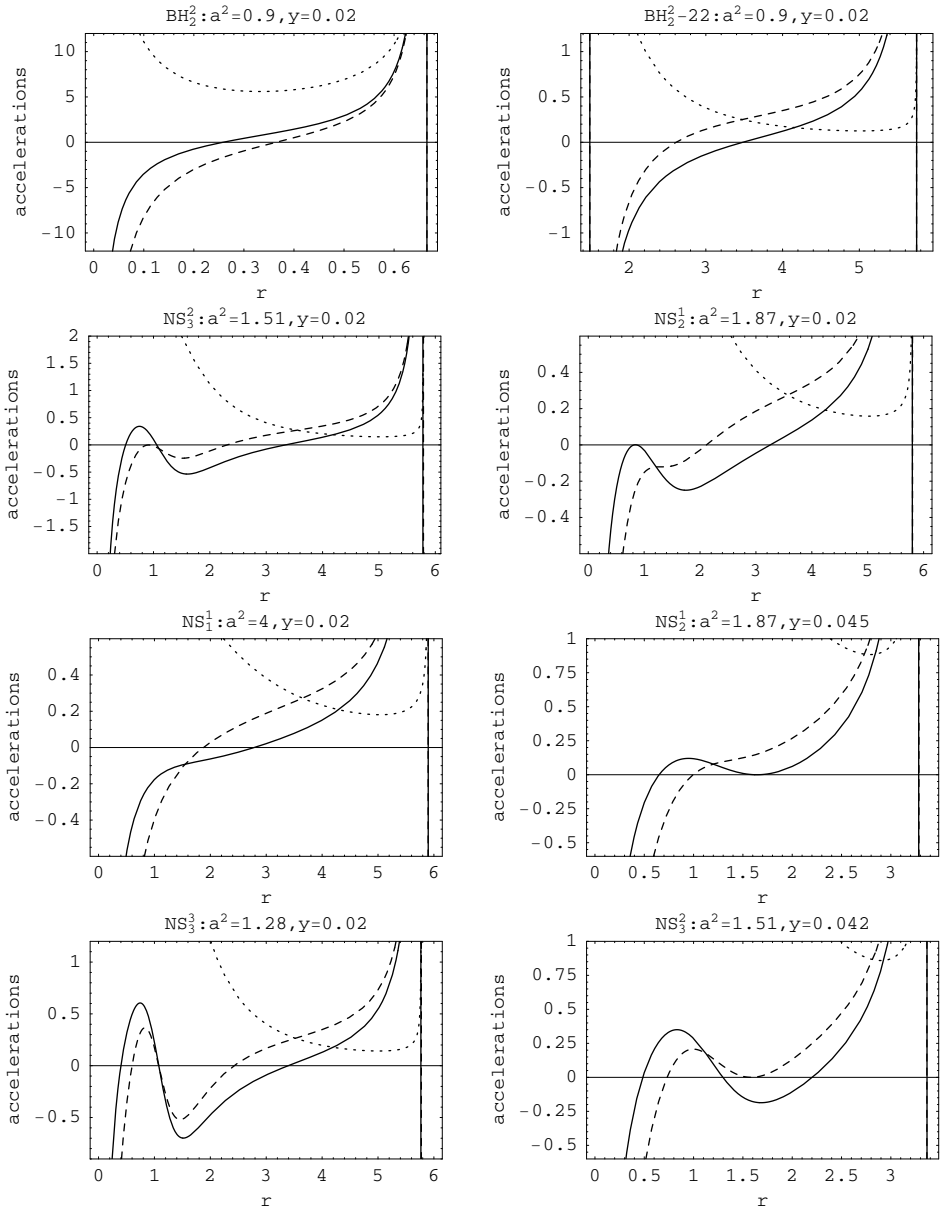

Figure 6. Gravitational acceleration $\mathcal{G}_r(r;a^2,y)$ (solid) and velocity independent parts of the centrifugal $\mathcal{Z}_r(r;a^2,y)$ (dashed) and Coriolis $\mathcal{C}_r(r;a^2,y)$ (dotted) accelerations of particles moving along circular orbits in the equatorial plane of the KdS spacetimes. There are examples of qualitatively different types of behaviour of $\mathcal{G}_r(r;a^2,y)$ and $\mathcal{Z}_r(r;a^2,y)$ corresponding to the presented classification of the spacetimes. Positive (negative) parts of $\mathcal{G}_r(r;a^2,y)$ and $\mathcal{Z}_r(r;a^2,y)$ determine repulsive (attractive) forces oriented outwards (towards) the singularity at $r=0$. The positive function $\mathcal{C}_r(r;a^2,y)$ determines the repulsive (attractive) Coriolis force in the case of the corotating orbits with $\tilde{v}>0$ (counterrotating orbits with $\tilde{v}<0$). The zero points of the functions determine the radii of circular orbits where the forces vanish independently of the velocity. The common points of $\mathcal{Z}_r(r;a^2,y)$ and $\mathcal{C}_r(r;a^2,y)$ determine the radii of counterrotating photon circular orbits. The vertical lines denote the radii of event horizons.

5. Relativistic dynamics in terms of forces

There are many interesting relativistic problems which can be investigated by using the inertial forces formalism. For example, choosing the description of the circular motion as an example in the equatorial plane, we can demonstrate that the formalism proves to be very effective and provides simpler and intuitive approach, as compared to the standard general relativistic methods. Another astrophysically relevant application of inertial forces formalism can be demonstrated by the determination of static equilibrium positions of test particles or of the perfect fluid equilibrium toroidal configurations. Therefore we believe that the inertial forces method, combined with the standard approaches, could bring in an effective way some new results in modelling accretion disks.

5.1. Equatorial circular orbits in general case

Acceleration necessary to keep a particle in an uniform circular motion in the equatorial plane ($v = const$, $\theta = \pi/2$) can be expressed due to relation (8) in the simple form [6], [15]

$$a_r^{\perp}(r, v) = -\mathcal{G}_r - (\gamma v)^2 \mathcal{Z}_r - \gamma^2 v \mathcal{C}_r, \tag{41}$$

or equivalently

$$a_r^{\perp}(r, \tilde{v}) = -\mathcal{G}_r - \tilde{v}^2 \mathcal{Z}_r - \tilde{v}(1 + \tilde{v}^2)^{1/2} \mathcal{C}_r, \tag{42}$$

where $-\infty < \tilde{v} < \infty$, while $-1 < v < 1$. These equations enable an effective discussion of the properties of both the accelerated and geodesic motions. Remind that there are only radial components of the inertial forces non-vanishing in the equatorial plane, the Euler force vanishes completely and $a_\theta^{\perp} = a_\phi^{\perp} = 0$.

For ultrarelativistic particles ($\tilde{v}^2 \gg 1$), we obtain from equation (41) the asymptotic equation

$$a_r^{\perp}(r, \tilde{v}) \approx -\mathcal{G}_r \mp \frac{1}{2}\mathcal{C}_r - \tilde{v}^2(\mathcal{Z}_r \pm \mathcal{C}_r), \tag{43}$$

for photons ($\tilde{v}^2 \to \infty$), the circular geodesics are determined by the equation

$$\mathcal{Z}_r \pm \mathcal{C}_r = 0, \tag{44}$$

where the upper signs correspond to the corotating motion ($\tilde{v} > 0$) and the lower signs to the counterrotating motion ($\tilde{v} < 0$). The ultrarelativistic particles moving along circular orbits at the radii of the photon circular orbits are kept by the acceleration

$$a_r^{\perp}(r) = -\mathcal{G}_r \mp \mathcal{C}_r, \tag{45}$$

which is velocity independent with the accuracy $O(\tilde{v}^{-2})$. In static spacetimes, there is $\mathcal{C}_r = 0$, and at the radius of the photon circular geodesic, the acceleration of particles is

$$a_r^{\perp}(r) = -\mathcal{G}_r, \tag{46}$$

which is velocity independent exactly. In this case, relation (46) is not limited to the case of ultrarelativistic particles, because $\mathcal{Z}_r = 0$ at the radius of the photon circular orbit in static spacetimes.

Velocities of particles moving along equatorial circular geodesics are due to relations (41), (42) and $a_r^{\perp}(r) = 0$ determined by the expressions

$$v_{\mp} = \frac{\mathcal{C}_r \mp (\mathcal{C}_r^2 - 4\mathcal{G}_r\mathcal{Z}_r + 4\mathcal{G}_r^2)^{1/2}}{2(\mathcal{G}_r - \mathcal{Z}_r)}, \tag{47}$$

or

$$\tilde{v}_{\pm} = \pm[\frac{\frac{1}{2}\mathcal{C}_r^2 - \mathcal{G}_r\mathcal{Z}_r \mp \frac{1}{2}\mathcal{C}_r(\mathcal{C}_r^2 - 4\mathcal{G}_r\mathcal{Z}_r + 4\mathcal{G}_r^2)^{1/2}}{\mathcal{Z}_r^2 - \mathcal{C}_r^2}]^{1/2}. \tag{48}$$

In more details, because of the relation $\tilde{v}^2 = (\gamma v)^2 = \frac{v^2}{1-v^2}$, we obtain from relation (47) the velocity $\tilde{v}$ in the form

$$\tilde{v}_{\pm} = \pm[\frac{\mathcal{G}_r^2}{\frac{1}{2}\mathcal{C}_r^2 - \mathcal{G}_r\mathcal{Z}_r \pm \frac{1}{2}\mathcal{C}_r(\mathcal{C}_r^2 - 4\mathcal{G}_r\mathcal{Z}_r + 4\mathcal{G}_r^2)^{1/2}}]^{1/2}, \tag{49}$$

which implies relation (48). It is clear that for the geodesic circular motion at a fixed radius, the condition

$$\mathcal{C}_r^2 - 4\mathcal{G}_r\mathcal{Z}_r + 4\mathcal{G}_r^2 > 0 \tag{50}$$

must be satisfied. Moreover, the condition

$$\frac{1}{2}\mathcal{C}_r^2 - \mathcal{G}_r\mathcal{Z}_r \pm \frac{1}{2}\mathcal{C}_r(\mathcal{C}_r^2 - 4\mathcal{G}_r\mathcal{Z}_r + 4\mathcal{G}_r^2)^{1/2} > 0 \tag{51}$$

following from relation (49), implies due to relation (48) the condition

$$\mathcal{Z}_r^2 - \mathcal{C}_r^2 > 0. \tag{52}$$

Hence, in static spacetimes §, where $\mathcal{C}_r = 0$, the reality condition for the circular geodesics is $\mathcal{G}_r\mathcal{Z}_r < 0$, i.e., the gravitational and centrifugal forces must point in opposite directions, in accordance with our intuition.

For the circular geodesics, the constants of motion, i.e., the specific energy E and angular momentum L of particle are given by the relations

$$E = -u^i\eta_i = \gamma[e^{\Phi} + v\Omega_{LNRF}(\xi^i\xi_i)^{1/2}], \tag{53}$$

$$L = u^i\xi_i = \gamma v(\xi^i\xi_i)^{1/2}. \tag{54}$$

The specific pseudo-energy $\tilde{E}$, defined in the Section 2 by the relation

$$\tilde{E} = -u^i\iota_i = \gamma e^{\Phi}, \tag{55}$$

is not conserved in general. It becomes the conserved quantity in static spacetimes only, where the vector field ι^i coalesces with the Killing vector field η^i.

5.2. Equatorial circular orbits in Kerr-de Sitter spacetimes

The velocity of a particle moving along a circular orbit in the equatorial plane (47) is in the KdS spacetimes given by the relation [41]

$$v_{\pm} = \frac{\pm[2a^2 + r(1 + a^2y)(r^2 + a^2)][r^{1/2}(1 - r^3y)^{1/2}] - a(a^2 + 3r^2)}{\Delta_r^{1/2}[r^3 - a^2(1 - r^3y)]}. \tag{56}$$

Solving equations (44), we directly obtain the relation for the photon circular orbits [41]

$$y^2a^4r^3 + 2ya^2r^2(r + 3) + r(r - 3)^2 - 4a^2. \tag{57}$$

In the equatorial plane, condition (50) directly implies the relation

$$\frac{4r^3y - 4}{-r\Delta_r} \geq 0, \tag{58}$$

giving the limit for the circular geodesics in the form $r \leq y^{-1/3} \equiv r_{sr}$, i.e., we immediately obtain the limit given by the so-called static radius [41]. The other condition for the existence of circular geodesics is then given by the relation

$$y^2a^4r^3 + 2ya^2r^2(r + 3) + r(r - 3)^2 - 4a^2 \geq 0. \tag{59}$$

Thus the circular equatorial geodesics are limited by the circular photon geodesics as well.

---

§ For comparison, the acceleration of particle moving uniformly along circular orbit in the equatorial (central) plane of the Schwarzschild spacetime is given by the relation

$$a_r^{\perp}(r, v) = -\mathcal{G}_r - (\gamma v)^2\mathcal{Z}_r = \frac{1 - (\gamma v)^2(r - 3)}{r^2 - 2r}.$$

Thus, in the case of the geodetical circular motion $a_r^{\perp}(r, v) = 0$, velocity of the particle is given by the relation

$$v_{\pm} = \pm\sqrt{\frac{1}{r - 2}}.$$

The only photon circular orbit, determined by the relation $\mathcal{Z}_r = 0$, where

$$\mathcal{Z}_r = \frac{r - 3}{r^2 - 2r},$$

is located at the radius $r = 3$, obtained from the limit $v \to 1$ as well. The necessary condition (50) implies the natural restriction $r > 0$ only, but condition (52) implies the limitation $r \geq 3$.

For example, considering now a rocket orbiting a Schwarzschild black hole, then at the radii $r > 3$, the rocket can orbit the black hole free, with the proper orbital velocity tuning the centrifugal force, oriented outward the black hole and balancing the attractive gravitational force. Increasing (decreasing) the orbital velocity, the centrifugal force increases (decreases) and the rocket leaves the orbit outward (inward) the black hole. At the radius $r = 3$, the rocket can orbit the black hole, but with their engines on, directed 'vertically' toward the black hole, in order to balance the gravitational force. Here, the centrifugal force vanishes independently of the velocity and thus the thrust of the engines is velocity independent. At the radii $r < 3$, the rocket can orbit the black hole, but as well as in the previous case, with engines on, balancing both the gravitational and centrifugal forces, both oriented toward the black hole. The thrust of the rocket depends on the chosen orbital velocity. Namely here, the rocket with a constant 'vertical' thrust of its engines, increasing (decreasing) the orbital velocity, the centrifugal force increases (decreases), but because of the opposite orientation of the centrifugal force, the rocket leaves the orbit inward (outward) the black hole.

6. Embedding diagrams

The analysis of the embedding diagrams ranks among the most fundamental techniques that enable us to understand phenomena present in extremely strong gravitational fields of black holes, naked singularities or other compact objects. The influence of spin, charge, magnetic field or cosmological constant on the structure of the spacetimes and their relation to the well known 'Schwarzschild throat' can be conveniently illustrated by embedding diagrams of 2-dimensional surfaces ($t = const$) of the ordinary geometry into the 3-dimensional Euclidean geometry. As for the illustrations of the features of the relativistic dynamics, the embedding diagrams of the optical reference geometry are more useful. Just the behaviour of inertial forces, especially the centrifugal force, describing the motion of test particles and photons in the framework of optical reference geometry, is directly imprinted into the structure of the embedding diagrams of the optical geometry.

6.1. General case

The general method of the embedding diagrams construction [17], [15] is following. In the 3-dimensional Euclidean space, with the line element expressed in the cylindrical coordinates (ρ, z, α) in the form

$$d\sigma^2 = d\rho^2 + \rho^2 d\alpha^2 + dz^2, \tag{60}$$

we can assume a surface with the line element

$$dl^2_{(E)} = [1 + (\frac{dz}{d\rho})^2]d\rho^2 + \rho^2 d\alpha^2. \tag{61}$$

Such surface is considered to be isometric to the 2-dimensional equatorial plane of the optical space, described by the line element

$$d\tilde{l}^2 = \tilde{h}_{rr}dr^2 + \tilde{h}_{\phi\phi}d\phi^2, \tag{62}$$

where $\tilde{h}_{rr}$ and $\tilde{h}_{\phi\phi}$ are metric coefficients of the optical geometry. Identifying the azimuthal coordinates ($\phi = \alpha$) and putting

$$\rho^2 = \tilde{h}_{\phi\phi}, \tag{63}$$

we obtain the embedding formula $z = z(\rho)$, characterizing the embedding diagram, in the differential form

$$(\frac{dz}{d\rho})^2 = \tilde{h}_{rr}(\frac{dr}{d\rho})^2 - 1. \tag{64}$$

It is convenient to rewrite the formula into the parametric form $z(\rho) = z(r(\rho))$ with r being the parameter, i.e.,

$$\frac{dz}{dr} = \pm\sqrt{\tilde{h}_{rr} - (\frac{d\rho}{dr})^2}, \tag{65}$$

whereas the sign in this formula is irrelevant, leading to isometric surfaces [18].

From the differential form of the embedding formula (65), it is clear that the optical geometry of the equatorial plane can not be entirely embeddable into the 3-dimensional

Euclidean space. The embeddable regions are determined by the condition $(dz/dr)^2 \geq 0$, whereas the equality in this relation determines the limits of embeddability.

In general, the plasticity of the embedding diagrams is characterized by the different steepness and by the turning points of the diagrams. Clearly, the turning points of the embedding diagrams, i.e., their bellies and throats, are determined by the relation $d\rho/dz = 0$. Because of the relation

$$\frac{dz}{d\rho} = \frac{dz}{dr}\frac{dr}{d\rho}, \tag{66}$$

we have the condition $d\rho/dr = 0$. Note that due to relations (4) and (63)

$$\rho^2 = \tilde{h}_{\phi\phi} = e^{-2\Phi} h_{\phi\phi}. \tag{67}$$

Moreover, due to relations (31) and (35), in the equatorial plane, we can write

$$\mathcal{Z}_r = \rho^{-1}\nabla_r \rho. \tag{68}$$

Thus it is clear that the turning points of the diagrams are located at the radii where the velocity independent part of the centrifugal acceleration vanishes, i.e., where

$$\mathcal{Z}_r = 0. \tag{69}$$

The radii of photon circular orbits are given by relations (44), i.e.,

$$\mathcal{Z}_r \pm \mathcal{C}_r = 0, \tag{70}$$

and then, of course, in the stationary (non-static) spacetimes, where $\mathcal{C}_r \neq 0$, the radii of photon circular orbits do not coalesce with the radii of the turning points of embedding diagrams, which holds for the static spacetimes, where $\mathcal{C}_r = 0$. Moreover, some of the photon circular orbits does not have to be embeddable.

6.2. Embedding of Kerr-de Sitter geometry

In the equatorial plane of the KdS geometry §, the needed metric coefficients of the optical reference geometry (4) are of the form

$$\tilde{h}_{rr} = \frac{r(1+a^2y)^2[2a^2 + a^2 r + r^3 + a^2 r(a^2+r^2)y]}{\Delta_r^2}, \tag{71}$$

$$\tilde{h}_{\phi\phi} = \frac{[2a^2 + a^2 r + r^3 + a^2 r(a^2+r^2)y]^2}{r^2\Delta_r}. \tag{72}$$

Using the metric coefficients and relation (63), we obtain the differential form of the embedding formula (65) in the form

$$\frac{dz}{dr} = \pm\sqrt{\frac{-L}{r^4\Delta_r^3}}, \tag{73}$$

where $L = Ay^4 + By^3 + Cy^2 + Dy + E$,

$$A = a^6 r^6 (a^2 + r^2)^3, \tag{74}$$

$$B = a^4 r^5 (a^2 + r^2)^2 [3r^3 + a^2(3r + 10)], \tag{75}$$

$$C = a^2 r^3 (a^2 + r^2)[3r^7 + a^2(6r^2 + 16r + 9)r^3 + a^4 r(3r^2 + 12r + 37) - 4a^6], \tag{76}$$

$$D = r^2\{r^{10} + a^2 r^6(3r^2 + 2r - 18) + a^4 r^3[r(3r^2 - 4r - 16) + 36] + a^6 r[r(r^2 - 14r - 18) + 60] - 4a^8(2r + 5)\}, \tag{77}$$

$$E = 4a^8 - 4a^6 r[r(r - 3) + 6] - 3a^4(r - 2)r^2[r(4r - 3) + 6] - a^2 r^5[r(6r - 17) + 18] + (9 - 4r)r^8. \tag{78}$$

6.3. Classification

The KdS spacetimes can be classified according to the main characteristics of the embedding diagrams, i.e., according to the number of embeddable regions, turning points of the embedding diagrams and the number of embeddable photon circular orbits (see Tab. 3 and Fig. 7). Some of the embedding diagrams are illustrated in Figs 8 and 9.

Table 3. Classification of the KdS spacetimes according to the number of embeddable regions (first digit), turning points of the embedding diagrams (second digit) and number of embeddable photon circular orbits (digit following dash).

	BH spacetimes	**NS spacetimes**
KdS	BH22-0, BH32-0	NS11-0, NS21-0, NS22-0, NS23-0, NS11-1, NS12-1
	BH22-1, BH22-2	NS13-1, NS21-1, NS22-1, NS23-1, NS33-1
Kerr	BH22-2, BH22-1	NS11-1, NS12-1, NS13-1, NS23-1, NS33-1
SdS	BH11-1	—
Schw	BH11-1	—

- KdS black-hole spacetimes contain three or two separated embeddable regions in contrast to the Kerr black-hole spacetimes, where only two regions occur, and to the SdS and Schwarzschild black-hole spacetimes with the only embeddable region.
- KdS naked-singularity spacetimes contain one, two or three separated embeddable regions as well as the Kerr naked-singularity spacetimes.
- KdS black-hole embedding diagrams contain two turning points as well as the Kerr black-hole diagrams. But the SdS and Schwarzschild black-hole embedding diagrams contain one turning point, coalescing with the radius of circular orbit where the centrifugal force vanishes independently of the velocity.
- KdS naked-singularity embedding diagrams contain one, two or three turning points as well as the Kerr naked-singularity diagrams.

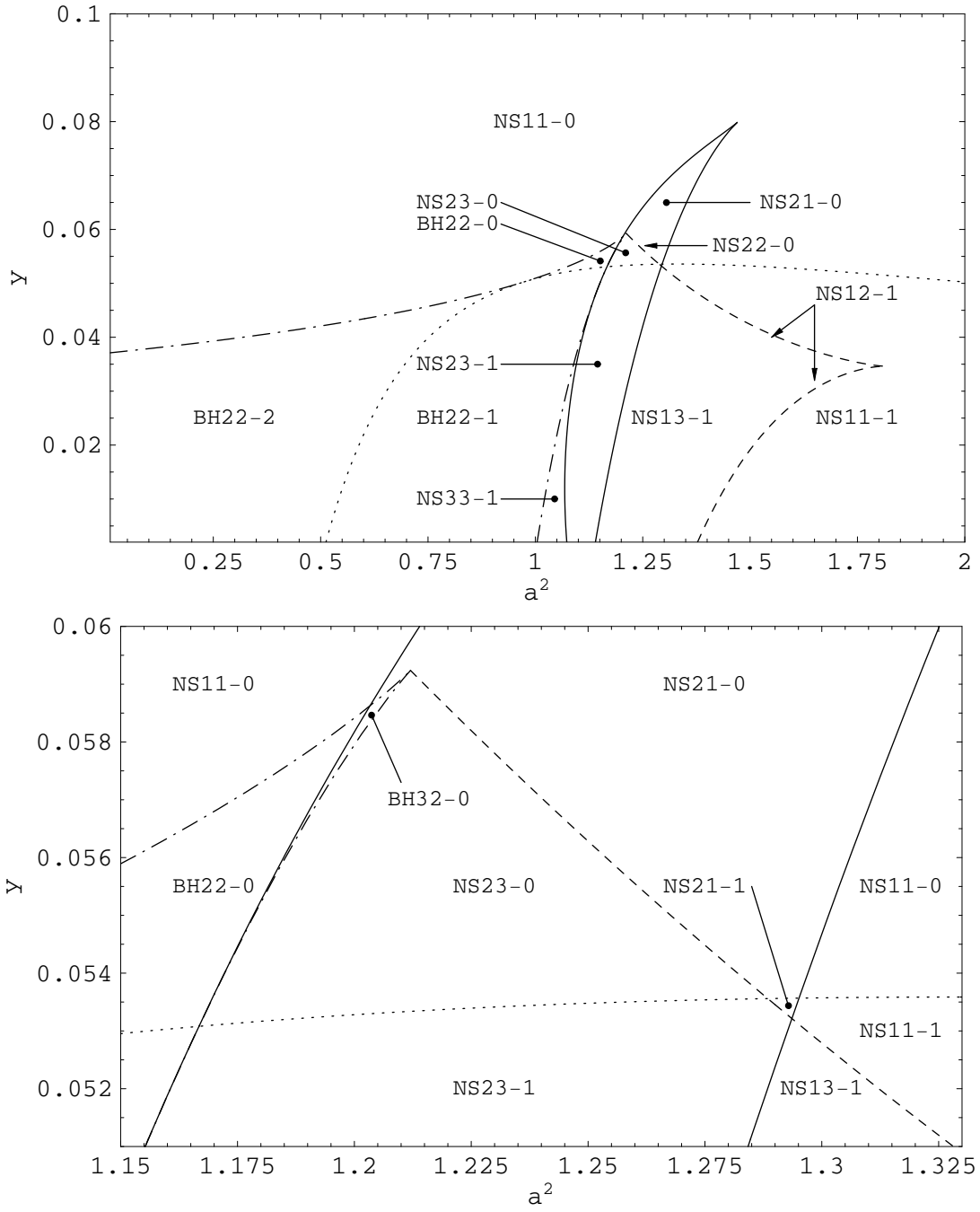

Figure 7. Classification of the KdS spacetimes. The parametric plane (a^2, y) is divided into regions corresponding to the classes differing in the number of embeddable regions (first digit), turning points of embedding diagrams (second digit) and embeddable photon circular orbits (digit following dash). Note that in the case of the classes NS12-1, NS22-1 and NS22-0, the second digits exceptionally denote one turning point and one inflexion point.

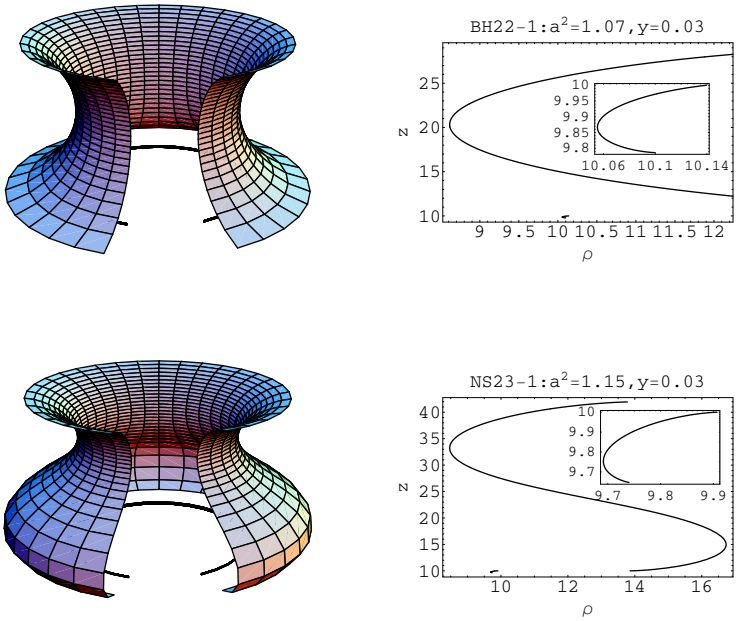

Figure 8. Embedding diagrams of the optical reference geometry of the KdS spacetime of the classes $BH22-1$ and $NS23-1$.

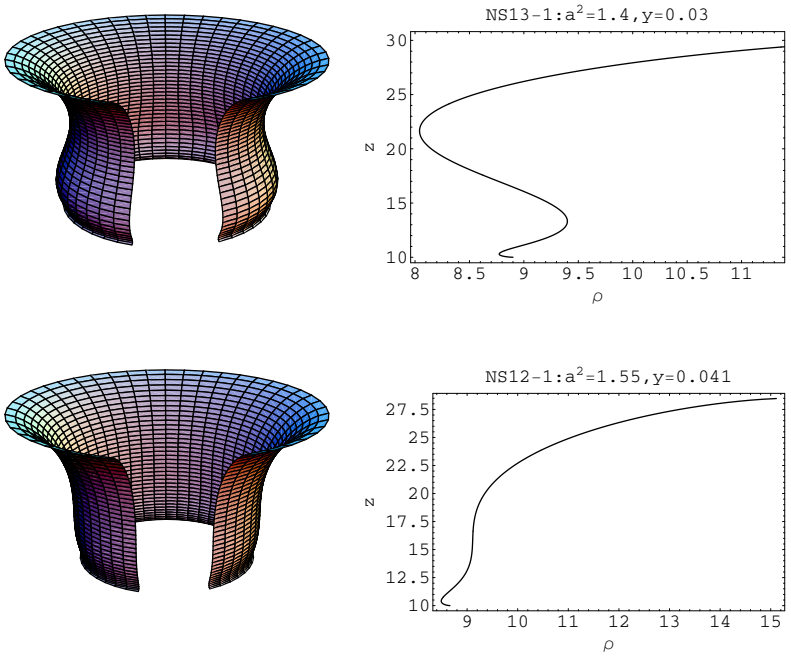

Figure 9. Embedding diagrams of the optical reference geometry of the KdS spacetime of the classes $NS13-1$ and $NS12-1$.

- KdS black-hole spacetimes contain three photon circular orbits, whereas two of them occur in the outer stationary region and one of them in the inner one as well as in the Kerr black-hole spacetimes, and in contrast to the SdS and Schwarzschild black-hole spacetimes, where only one orbit occurs.
- KdS naked-singularity spacetimes contain one photon circular orbit as well as the Kerr naked-singularity spacetimes.
- KdS black-hole spacetimes contain two, one or none embeddable photon circular orbits in the outer stationary region in contrast to the Kerr black-hole spacetimes, where always two or one embeddable orbits exist, and to the SdS and Schwarzschild black-hole spacetimes, where always one embeddable orbit occurs at the radius coalescing with the radius of turning point of the embedding diagram.
- KdS naked-singularity spacetimes contain one or none embeddable photon circular orbit in contrast to the Kerr naked-singularity spacetimes, where always one embeddable orbit occurs.

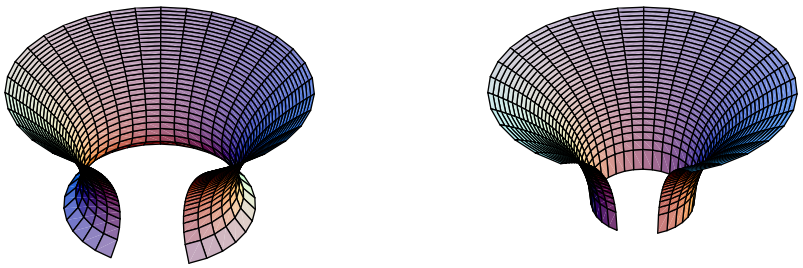

Figure 10. Embedding diagrams of the optical reference geometry (left) and ordinary geometry (right) of the Schwarzschild spacetime.

§ The embedding diagram of the ordinary Schwarzschild geometry is determined by the embedding formula

$$\frac{dz}{dr} = \sqrt{\frac{2}{r-2}},$$

whereas the static region $r > 2$ of the geometry is whole embeddable and there are no turning points of the diagram.

The embedding formula for the optical reference geometry (65) takes the form

$$\frac{dz}{dr} = \sqrt{\frac{r(4r-9)}{(r-2)^3}},$$

and the geometry of the static region of the Schwarzschild spacetimes is not whole embeddable, there is a limit of embeddability. The geometry is embeddable only at the radii $r > 9/4$. Because of relation (69), there is one turning point of the embedding diagram, corresponding to the radius of the photon circular orbit located at $r = 3$ (see Fig. 10).

7. Conclusion

As far as I know, there are many papers concerning the optical reference geometry and inertial forces formalism. But unfortunately, each of them covers only a narrow part of the entire formalism. Moreover, there are slightly different initial definitions of the formalism and some of the papers contain typographical mistakes in the basic formulas, which can be misleading for someone. Thus first of all, in sum the thesis should provide the basic and overall unified view of the formalism and its practical applications on the background of the Kerr-de Sitter spacetimes and its limit cases, i.e., of the Kerr, Schwarzschild-de Sitter and Schwarzschild spacetimes, introduced as well in the original papers [26], [29] and [24], prepared with a collaboration with my supervisor, Prof. RNDr. Zdeněk Stuchlík, CSc. The thesis should also demonstrate that the inertial forces formalism and embedding diagrams of the optical geometry, omitting the general relativistic definition and technical details, are illustrative and simply enough, and ready to be used even by students of physics untrained in general relativity for investigation of some interesting problems of black-hole physics. In particular, it could and it does provide to experts an useful and intuitive alternative tool, either for an initial research or for comparisons and verification. Thus the work could be also considered as an introduction in developing a new approach to study of the astrophysical phenomena in strong gravitational fields. Finally, experts in the optical reference geometry could appreciate extension of the formalism to the wide range of astrophysically relevant compact objects spacetimes described by the Kerr-de Sitter solution of Einstein's equations, and the technical aspects. In general, from the other point of view, the thesis reports about some new facts concerning the general topic 'The role of cosmological constant in relativistic physics and astrophysics', heavily discussed these days .

References

[1] Abramowicz M A, Carter B and Lasota J 1988 *Gen. Relativity Gravitation* **20** 1173
[2] Abramowicz M A and Prasanna A R 1990 *Royal Astronomical Society Monthly Notices* **245** 720
[3] Abramowicz M A and Miller J 1990 *Royal Astronomical Society Monthly Notices* **245** 729
[4] Abramowicz M A, Nurowski P and Wex N 1993 *Classical Quantum Gravity* **10** L183
[5] Abramowicz M A 1993 *The Renaissance of General Relativity and Cosmology* (Cambridge University Press) 40-58
[6] Abramowicz M A, Nurowski P and Wex N 1995 *Classical Quantum Gravity* **12** 1467
[7] Sonego S and Massar M 1996 *Classical Quantum Gravity* **13** 139
[8] Jonsson R 2006 *Classical Quantum Gravity* **23** 1
[9] Stuchlík Z 1990 *Bull. Astronom. Inst. Czechoslovakia* **41** 341
[10] Stuchlík Z and Hledík S 1999 *Physical Review D* **60** 044006
[11] Kristiansson S, Sonego S and Abramowicz M A 1998 *Gen. Relativity Gravitation* **30** 275
[12] Stuchlík Z and Hledík S 2002 *Acta Phys. Slovaca* **52** 363
[13] Iyer S and Prasanna A R 1993 *Classical Quantum Gravity* **10** L13
[14] Stuchlík Z and Hledík S 1999 *Acta Phys. Slovaca* **49** 795
[15] Stuchlík Z, Hledík S and Juráň J 2000 *Classical Quantum Gravity* **17** 2691
[16] Stuchlík Z and Hledík S 1999 *Classical Quantum Gravity* **16** 1377
[17] Hledík S 2002 *Gravitation: Following the Prague Inspiration (A Volume in Celebration of the 60th Birthday of Jiří Bičák)* (World Scientific)
[18] Hledík S 2001 *Proceedings of RAGtime 2/3: Workshops on black holes and neutron stars, Opava, 11–13/8–10 October 2000/01* (Silesian University in Opava, Czech Republic)
[19] Aguirregabiria J M, Chamorro A, Nayak Rajesh K, Suinaga J and Vishveshwara C V 1996 *Classical Quantum Gravity* **13** 2179
[20] Nayak Rajesh K and Vishveshwara C V 1996 *Classical Quantum Gravity* **13** 1783
[21] Slaný P and Stuchlík Z 2005 *Classical Quantum Gravity* **22** 3623
[22] Stuchlík Z 2005 *Modern Physics Lett. A* **20** 561
[23] Stuchlík Z and Slaný P 2004 *Phys. Rev. D* **69** 064001
[24] Stuchlík Z and Kovář J 2006 *Classical Quantum Gravity* **23** 3935
[25] Kovář J and Stuchlík Z 2004 *Proceedings of RAGtime 4/5: Workshops on black holes and neutron stars, Opava, 14–16/13–15 October 2002/03* (Silesian University in Opava, Czech Republic)
[26] Kovář J and Stuchlík Z 2006 *International Journal of Modern Physics A* **21** (in print)
[27] Abramowicz M A, Miller J C and Stuchlík Z 1993 *Phys. Rev. D* **47** 1440
[28] Nayak Rajesh K and Vishveshwara C V 1998 *General Relativity and Gravitation* **30** 593
[29] Kovář J and Stuchlík Z 2006 *Classical Quantum Gravity* (being reviewed)
[30] Aguirregabiria J M, Chamorro A, Suinaga J and Vishveshwara C V 1995 *Classical Quantum Gravity*, **12** 699
[31] Balek V, Bičák J and Stuchlík Z 1989 *Bull. Astronom. Inst. Czechoslovakia*, **40** 133
[32] Bičák J, Stuchlík Z and Balek V 1989 *Bull. Astronom. Inst. Czechoslovakia*, **40** 65
[33] Bonnor W B 1993 *Classical Quantum Gravity*, **10** 2077
[34] Misner C W, Thorne K S and Wheeler J A 1973 *Gravitation* (Freeman, San Francisco)
[35] Papapetrou A 1951 *Proc. Roy. Soc. London Ser. A* 209
[36] Pirani R A E 1956 *Acta Phys. Polon. A* **15** 389
[37] Stuchlík Z 1999 *Acta Phys. Slovaca* **49** 319
[38] Stuchlík Z, Bičák J and Balek V 1999 *Gen. Relativity Gravitation* **31** 53
[39] Stuchlík Z and Hledík S 1999 *Phys. Rev. D* **60** 044006
[40] Stuchlík Z and Hledík S 2001 *Phys. Rev. D* **64** 104016
[41] Stuchlík Z and Slaný P 2004 *Phys. Rev. D* **69** 064001

Author's publications

Kovář J. and Stuchlík Z. 2004, **Inertial forces in Kerr-de Sitter spacetimes** *Proceedings of RAGtime 4/5: Workshops on black holes and neutron stars, Opava, 14–16/13–15 October 2002/03* (Silesian University in Opava, Czech Republic)

Kovář J. and Stuchlík Z. 2005, **Embedding diagrams of optical reference geometry of Kerr-de Sitter spacetimes** *Proceedings of RAGtime 6/7: Workshops on black holes and neutron stars, Opava, 16–18/18–20 September 2004/05* (Silesian University in Opava, Czech Republic)

Stuchlík Z. and Kovář J. 2005, **Equilibrium of spinning test particles in equatorial plane of Kerr-de Sitter spacetimes** *Proceedings of RAGtime 6/7: Workshops on black holes and neutron stars, Opava, 16–18/18–20 September 2004/05* (Silesian University in Opava, Czech Republic)

Schovancová J., Šubr L., Karas V., Stuchlík Z. and Kovář J. 2005, **Some aspects of the Störmer problem in strong gravitational fields** *Proceedings of RAGtime 6/7: Workshops on black holes and neutron stars, Opava, 16–18/18–20 September 2004/05* (Silesian University in Opava, Czech Republic)

Kovář J. and Stuchlík Z. 2006, **Forces in Kerr spacetimes with a repulsive cosmological constant** *International Journal of Modern Physics A* **21** (in print)

Stuchlík Z. and Kovář J. 2006, **Equilibrium conditions of spinning test particles in Kerr-de Sitter spacetimes** *Classical Quantum Gravity* **23** 3935

Kovář J. and Stuchlík Z. 2006, **Optical reference geometry of Kerr-de Sitter spacetimes** *Classical Quantum Gravity* (being reviewed)

Kovář J .and Stuchlík Z. 2006, **Optical reference geometry of Kerr-de Sitter spacetimes** *Proceedings of 11th Marcel Grossmann meeting, Berlin, June 23-29, 2006* (in preparation for World Scientific)

Author's conference contributions

Inertial forces in Kerr-de Sitter spacetimes
RAGtime 5: Workshops on black holes and neutron stars - Oral presentation
Opava, 2003

Embedding diagrams of optical reference geometry of Kerr-de Sitter spacetimes
RAGtime 6: Workshops on black holes and neutron stars - Oral presentation
Opava, 2004

Equilibrium of spinning test particles in equatorial plane of Kerr-de Sitter spacetimes
RAGtime 7: Workshops on black holes and neutron stars - Oral presentation
Opava, 2005

Equilibrium of spinning test particles in Kerr-de Sitter spacetimes
Albert Einstein Century Conference - Poster presentation
Paris, 2005

Optical reference geometry of Kerr-de Sitter spacetimes
Albert Einstein Century Conference - Poster presentation
Paris, 2005

Optical reference geometry of Kerr-de Sitter spacetimes
11th Marcel Grossmann Meeting - Oral presentation
Berlin, 2006

Doktorská disertační práce byla vypracována formou kombinovaného studijního programu na Katedře optiky Přírodovědecké fakulty Univerzity Palackého v Olomouci.

Uchazeč:	Mgr. Jiří Kovář
Školitel:	Prof. RNDr. Zdeněk Stuchlík, CSc. Ústav fyziky, Filozoficko-přírodovědecká fakulta, Slezská Univerzita v Opavě.
Konzultant:	RNDr. Stanislav Hledík, Ph.D. Ústav fyziky, Filozoficko-přírodovědecká fakulta, Slezská Univerzita v Opavě.
Oponenti:	Prof. RNDr. Jan Novotný, CSc. Katedra obecné fyziky, Přírodovědecká fakulta, MU Brno
	Doc. RNDr. Vladimír Karas, DrSc. Astronomický ústav Akademie věd ČR, Praha
	Mgr. Lukáš Richterek, Ph.D. Katedra teoretické fyziky, Přírodovědecká fakulta, UP Olomouc

Stanovisko o disertační práci vypracovala Katedra optiky Přírodovědecké fakulty Univerzity Palackého v Olomouci.

Autoreferát byl rozeslán dne: ..... .

Obhajoba disertační práce se koná dne ..... v ..... hodin před komisí pro obhajobu disertační práce vědního oboru fyzika, číslo P1701, studijního oboru *Obecná fyzika a matematická fyzika* v ....

S disertační prací je možné se seznámit v knihovně Přírodovědecké fakulty UP Olomouc.